Gray and White Matter Alterations in Early HIV-Infected Patients: Combined Voxel-Based Morphometry and Tract-Based Spatial Statistics

Bo Wang, PhD,[1,2†] Zhenyu Liu, PhD,[2†] Jiaojiao Liu, MD,[3†] Zhenchao Tang, PhD,[4] Hongjun Li, MD,[3*] and Jie Tian, PhD[2*]

Purpose: To investigate both the gray matter (GM) and whiter matter (WM) alterations in a homogeneous cohort of early HIV-infected patients by combining voxel-based morphometry (VBM) and tract-based spatial statistics (TBSS).
Materials and Methods: Twenty-six HIV and 26 control subjects enrolled in this study with 3D T_1 and diffusion-tensor imaging acquired on a 3.0T Siemens scanner. Group differences in regional GM were assessed using VBM analysis, while differences in fractional anisotropy (FA), mean diffusivity (MD), axial diffusivity (AD), and relative anisotropy (RD) of WM were evaluated using TBSS analysis. After that, interactions between GM changes and white matter alterations were investigated by using a correlation analysis.
Results: The HIV-infected patients displayed decreased GM volume, mainly located in the bilateral frontal cortices, bilateral anterior cingulate cortex, and left supplementary motor area ($P < 0.05$, false discovery rate-corrected). Meanwhile, the patient group showed decreased FA in the genu of capsule callosum, body of capsule callosum, and bilateral anterior corona radiate ($P < 0.05$, family wise error [FEW]-corrected). Areas of increased MD, RD, and AD in HIV patients were more extensive and observed in most skeleton locations ($P < 0.05$, FEW-corrected). The interaction analysis in the patient group revealed that there were no significant correlations between GM changes and WM alterations ($P > 0.05$).
Conclusion: Our results indicate that structural brain alterations occurred early in HIV-infected patients. The current study may shed further light on the potential brain effects of HIV.

J. MAGN. RESON. IMAGING 2016;43:1474–1483.

Acquired immune deficiency syndrome (AIDS) is a disease spectrum of the human immune system caused by infection with human immunodeficiency virus (HIV).[1] Although it has been established that HIV invasion of the brain occurs soon after initial infection, possible brain changes during this period are not well characterized.[2] The most common histopathological findings in autopsy studies of HIV-infected patients show that brain atrophy, white matter alterations, demyelination, and injury to subcortical regions, occur in the later stages of infection.[3–5] HIV-associated neurocognitive disorders (HAND) and HIV-associated dementia (HAD) have been strongly associated with an increased risk of death.[6] However, the onset of a neurologic disorder still has not been determined.[7] Therefore, a clearer understanding of brain injury with HIV infection, particularly in the early stages, is critical.

Magnetic resonance imaging (MRI) provides a noninvasive examination of brain structure changes in HIV infection.[8] Diffusion tensor imaging (DTI) is one of the most rapidly evolving MRI techniques, which is more sensitive in detecting subtle white matter (WM) changes.[9] Derived from DTI, changes in four parameters, including fractional

View this article online at wileyonlinelibrary.com. DOI: 10.1002/jmri.25100

Received Jul 31, 2015, Accepted for publication Nov 3, 2015.

*Address reprint requests to: J.T., Floor 9, Intelligent Building, No. 95, Zhongguancun East Road, Haidian District, Beijing, China. E-mail: tian@ieee.org or H.L., No. 8, Xi Tou Tiao, Youanmen wai, Fengtai District, Beijing, China. E-mail: lihongjun00113@126.com

The first three authors contributed equally to this work.

From the [1]School of Automation, Harbin University of Science and Technology, Harbin, China; [2]Key Laboratory of Molecular Imaging, Chinese Academy of Sciences, Beijing, China; [3]Radiology Department, You'an Hospital of Capital Medical University, Beijing, China; and [4]School of Mechanical, Electrical & Information Engineering, Shandong University, Weihai, China

anisotropy (FA), mean diffusivity (MD), axial diffusivity (AD), and radial diffusivity (RD), may reflect microstructural abnormality of WM.[9] Using a region of interest (ROI)-based method, brain abnormalities have been reported in multiple regions in HIV-infected patients, including the genus of corpus callosum,[10–12] frontal WM,[13–15] hippocampi,[10] lentiform nucleus,[11] temporal WM,[14] internal capsule,[13] basal ganglia,[15] parietal and periventricular WM.[11] Besides ROI-based analysis, there were also many studies of WM abnormality using whole-brain-based DTI analysis.[16–19]

In addition, another MRI analysis method called voxel-based morphometry (VBM) has revealed widespread gray matter (GM) and WM changes in HIV patients.[20] A recent VBM study by Küper et al showed that HIV leads to regional atrophy of cerebral GM and WM structures, which particularly affected nigrostriatal and frontostriatal circuits when comparing HIV-positive individuals with concomitant cognitive decline with controls.[21] More recently, Sarma et al investigated the regional brain GM and WM changes in perinatally HIV-infected adolescents receiving antiretroviral therapy (ART) with VBM analyses.[22] They showed that both decreased WM and increased GM volume appeared in perinatally HIV-infected youths for several brain regions when compared to controls.

Although many previous studies have reported brain alterations in patients with HIV, few studies focused on the early stages of HIV infection. In this study we sought to characterize possible brain changes during the early period of HIV-infection by combining VBM and tract-based spatial statistics (TBSS).[23] In taking this approach, our study had two primary goals. First, we tried to detect GM and WM alterations in the early HIV-infected patients, where mean length of infection was estimated as less than 1 year based on assay results. Second, we sought to investigate the interactions between GM changes and WM alterations through a correlation analysis.

Materials and Methods

This study was approved by the Beijing You'an Hospital of Capital Medical University. All participants provided written informed consent.

Subjects

Twenty-six HIV-infected patients (23 males, 3 females; mean age: 38.0 ± 11.3 years) and 26 healthy controls (19 males, 7 females; mean age: 34.0 ± 9.4 years) were enrolled in our study. The inclusion criteria for patients were: all of their mean length of infection was estimated as less than 1 year based on assay results, and HAD stage was 0 or 0.5. Exclusion criteria for all the subjects included any drug abuse history and any obvious brain lesions, such as stroke or tumors assessed on the basis of medical history and conventional MRI. All healthy controls were enrolled from the same urban areas as the infected subjects. Demographic and clinical information of HIV-infected and control subjects are presented in Tables 1 and 2.

Data Acquisition

All MRIs were acquired on a 3.0T Siemens scanner (Allegra, Siemens Medical System, Erlangen, Germany) at the Beijing You'an Hospital of Capital Medical University. A standard birdcage head coil was used, along with restraining foam pads to minimize head motion and to diminish scanner noise. First, high-resolution 3D T_1-weighted images (T_1WI) were obtained with a spoiled gradient recall sequence and the following parameters: repetition time (TR) = 1900 msec; echo time (TE) = 2.52 msec; field of view (FOV) = 250 × 250 mm; in-plane matrix = 256 × 256; slice thickness = 1 mm; number of slices = 176; acquisition time (TA) = 4.18 minutes. Second, DTIs were obtained along 20 non-collinear directions with $b = 1000$ s/mm^2 and one $b = 0$ s/mm^2. The parameters were: TR/TE = 3300/90 msec; slice thickness = 4 mm; number of slice = 63; FOV = 230 × 230 mm; acquisition matrix = 128 × 128; number of excitation (NEX) = 3; TA = 3.39 minutes.

Data Processing

For T_1-weighted images, VBM processing was performed with the VBM8 toolbox (http://dbm.neuro.uni-jena.de/vbm8/) which runs within the statistical parametric mapping package (SPM8, http://www.fil.ion.ucl.ac.uk/spm/). VBM involves a voxel-wise comparison of the local concentration of GM between two groups of subjects. Our processing included three steps. First, T_1-weighted images were corrected for any bias, and partitioned into GM, WM, and cerebrospinal fluid (CSF) tissue types using a unified segmentation approach.[24] GM and WM were normalized to the standard Montreal Neurological Institute (MNI) space with linear (12-parameter affine) and nonlinear transformation (warping). Second, analysis was performed on GM tissue separately, which was multiplied by the nonlinear components derived from the normalization matrix in order to preserve actual GM value locally (modulated GM volume). Finally, the modulated volumes were smoothed using an isotropic Gaussian kernel of 6 mm full-width at half maximum (FWHM).[25]

For DTI images, TBSS processing was performed with FSL5.0 (FMRIB Image Analysis Group, Oxford, UK, http://www.fmrib.ox.ac.uk/fsl). Our analysis involved two stages. The first stage was to create FA data from DTI data. First, the DTI was corrected for the effects of eddy currents and head movement using eddy current correction within FDT (FMRIB's Diffusion Toolbox, part of FSL). Then brain masks were extracted by running BET (Brain Extraction Tool, part of FSL) on one of the no diffusion weighting ($b = 0$) images.[26] After eddy current correction and brain extraction, the diffusion tensor model at each voxel was fit using DTIFIT within FDT. With this, several DTI measures including FA, MD, AD, and RD can be derived from the tensor. The next stage is TBSS processing. As FA is a normalized measure of eigenvalue standard deviation and represents the degree of diffusion directionality,[27] we analyzed the FA data using TBSS with the following four steps[23]: first, a common registration target was identified and all subjects' FA images were aligned to this target using FNIRT (FMRIB's Nonlinear Image Registration Tool, part of FSL), which

TABLE 1. Clinical Data of Patients

Subject	Age	Sex	Medication	Start-of-medication	CD4 (cells/μl)	HAD stage
1	38	M	none	en	405	0
2	29	M	none	en	11	0
3	40	M	HAART	lm	45	0
4	36	M	none	en	39	0
5	38	F	HAART	lm	334	0
6	45	M	none	en	174	0
7	38	M	none	en	8	0
8	30	M	HAART	lm	385	0
9	28	M	none	en	214	0
10	27	M	none	en	273	0
11	37	M	none	en	532	0
12	37	F	HAART	lm	702	0
13	44	M	HAART	lm	368	0
14	28	M	HAART	em	679	0
15	58	M	none	en	400	0
16	21	M	none	en	332	0
17	31	M	none	en	734	0
18	35	M	HAART	em	80	0
19	63	M	none	en	279	0
20	50	M	none	en	279	0
21	39	M	none	en	32	0
22	60	M	HAART	em	47	0
23	49	M	HAART	lm	190	0
24	27	M	none	en	260	0
25	19	M	none	en	67	0
26	42	F	none	en	134	0.5

M, male; F, female; HAART highly active antiretroviral therapy; lm, later with medication; em, early with medication; en, early without medication; HAD, HIV-associated dementia.

uses a *b*-spline representation of the registration warp field[28]; second, the mean of all aligned FA images were created and applied thinning to create a mean FA skeleton image (threshold = 0.2); third, each subject's aligned FA image was projected onto the mean FA skeleton by filling the skeleton with FA values from the nearest relevant tract center; fourth, voxel-wise cross-subject statistical analyses of FA were carried out on the skeleton space. Furthermore, we also performed TBSS analysis on non-FA parameters, including MD, AD, and RD.

Statistical Analysis

For VBM, a two-sample *t*-test based on the random effect model was performed voxel-wise to determine the differences in GM volume between HIV + patients and healthy controls, with age and gender as covariates of no interest to exclude the possible effect of these variables on regional GM volume. Significance was set at $P < 0.05$, corrected for false discovery rate (FDR). A contiguous cluster of at least 20 voxels was accepted as significant. Significant clusters with a volume at least 100 mm^3 were superimposed on an MNI template.

For TBSS, a voxel-wise permutation-based ($n = 10{,}000$) nonparametric test was applied to compare the FA maps of HIV + patients and controls using the Randomize tool in FSL (http://www.fmrib.ox.ac.uk/fsl/randomise/). Significance was set at $P < 0.05$, corrected for family-wise error (FEW) using threshold-free cluster enhancement.[29] The preprocessing and groups analyses were also performed on non-FA maps, including MD, AD, and RD. The Johns Hopkins University ICBM-

TABLE 2. Clinical and Demographic Characteristics of Study Participants

Items	HIV + patients	Healthy controls	*P*-value
N	26	26	N/A
age	38.0 ± 11.3	34.0 ± 9.4	0.18*
sex (M / F)	23/3	19/7	0.17*
CD4 count	255 ± 220	N/A	N/A
CD4 > 200 (%)	50 (*N* = 13)	N/A	N/A

N number of subjects; *$P > 0.05$; M, male; F, female; N/A not applicable or available.

DTI-81 White Matter Atlas[30] was used to label significant tracts.

To investigate the interactions between GM changes and WM alterations, a correlation analysis was performed between abnormal GM volumes and WM FA values in the HIV-infected group.

Results

There was no significant difference for age and gender between the HIV + patient and healthy control groups (all $P > 0.05$) (Table 2).

VBM Results

Compared with healthy controls, significantly decreased GM in HIV-infected patients was present in the bilateral frontal cortices (ie, the bilateral superior frontal gyrus, the left middle frontal gyrus, and the left inferior frontal gyrus), the bilateral anterior cingulate cortex (ACC), and the left supplementary motor area (SMA) ($P < 0.05$, FDR-corrected). In addition, GM volumes of the frontal cortices, the ACC, and the left SMA showed a positive correlation with CD4 counts, but no significance ($r1 = 0.1229$, $P1 > 0.05$; $r2 = 0.2478$, $P2 > 0.05$; $r3 = 0.1170$, $P3 > 0.05$). The results are illustrated in Fig. 1 and Table 3.

TBSS Results

Compared with healthy controls, the HIV-infected patients showed decreased FA and increased MD, RD, and AD in

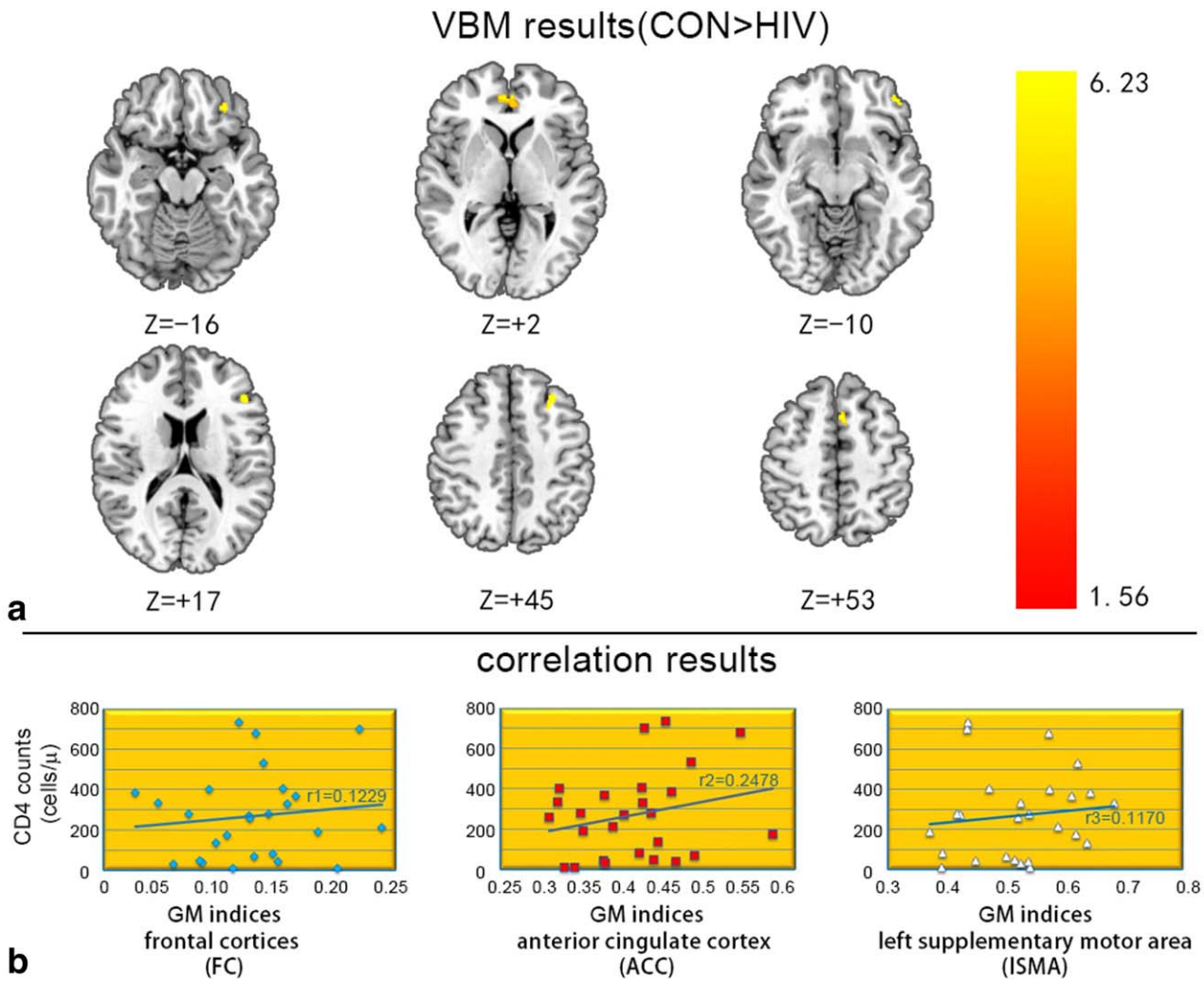

FIGURE 1: Voxel-based morphometry (VBM) results of the healthy controls vs. HIV infection group comparison.

TABLE 3. Regions Showing Decreased Gray Matter (GM) Between HIV-Infected Patients and Healthy Controls

Cluster	Regions	Hemisphere	BA	number of voxels	Peak *t* value	Peak MNI coordinates		
						x	y	z
1	Frontal_Inf, Frontal_Mid_Orb	L	47,11	51	5.20	−31	38	−16
2	Frontal_Sup_Medial; Cingulum_Ant, Frontal_Sup_Orb	R L / R	10 10,11	1403	6.23	4	47	2
3	Frontal_Inf_Orb	L	47	53	4.89	−44	45	−10
4	Frontal_Inf_Tri	L	45,48	78	5.30	−47	30	17
5	Frontal_Mid	L	9	78	5.19	−32	30	45
6	Supp_Motor_Area	L	32,6	99	5.48	−3	14	53

Positive value in the peak *t*-score represents a decrease in brain volume (control > patient).
All $P < 0.05$, FDR-corrected; the minimal cluster size is 100 mm^3 (30 voxels). R, right; L, left; MNI, Montreal Neurological Institute; BA, Brodmann's area; Frontal_Inf, Inferior Frontal Gyrus; Frontal_Mid_Orb, Middle Frontal Gyrus, orbital; Frontal_Sup_Medial, Superior Frontal Gyrus, medial; Cingulum_Ant, Cingulum Ant; Frontal_Sup_Orb, Superior Frontal Gyrus, orbital; Frontal_Inf_Orb, Inferior Frontal Gyrus, orbital; Frontal_Inf_Tri, Inferior Frontal Gyrus, triangular; Frontal_Mid, Middle Frontal Gyrus; Supp_Motor_Area, Supplementary Motor Area.

multiple brain regions ($P < 0.05$, FEW-corrected). No region showed increased FA or decreased MD, RD, or AD in the patients ($P < 0.05$, FEW-corrected). In addition, FA values of the genu of capsule callosum (GCC), the bilateral anterior corona radiate (ACR) showed a positive correlation with CD4 counts ($r4 = 0.2251$, $P4 > 0.05$; $r6 = 0.2538$, $P6 > 0.05$; $r7 = 0.3471$, $P7 > 0.05$), whereas negative correlation between FA of body of capsule callosum (BCC) and CD4 counts ($r5 = –0.3376$, $P5 > 0.05$). However, none of those correlations were significant (all $P > 0.05$). The results are illustrated in Fig. 2.

The location and cluster size (clusters >100 voxels) of the WM tracts where FA, MD, RD, and AD showed significant between-group differences are summarized in Table 4. In detail, the HIV-infected patients showed decreased FA in the GCC, BCC, and bilateral ACR when compared to the control group ($P < 0.05$, FEW-corrected) (Fig. 2, Table 4). In contrast, increased MD were found in the GCC, BCC, bilateral ACR, splenium of corpus callosum (SCC), bilateral anterior limb of internal capsule (ALIC), external capsule (EC), posterior thalamic radiation (PTR), superior longitudinal fasciculus (SLF), posterior corona radiate (PCR), superior corona radiate (SCR), bilateral section of cingulum around cingulate gyrus, right retrolenticular part of internal capsule (RIC), right superior fronto-occipital fasciculus (SFOF), and right tapetum ($P < 0.05$, FEW-corrected) (Fig. 2, Table 4). In addition, an elevated RD value was observed in most skeleton locations that exhibited significantly increased MD within HIV-infected group ($P < 0.05$, FEW-corrected). However, areas of increased AD were much less prevalent when compared with either MD or RD (Fig. 2, Table 4).

Interaction Between GM and WM Abnormalities

The interaction analysis between GM and WM abnormalities in HIV-infected group revealed that there were no significant correlations between these two measures ($P > 0.05$) (Fig. 3).

Discussion

In this study we evaluated both the GM and WM changes of HIV-infected patients during the early stage by combining the VBM and TBSS. The results showed decreased GM accompanied by WM microstructural abnormalities in HIV-infected patients when compared to the healthy controls.

For GM changes in HIV infection, our study demonstrated that decreased GM volume occurred in several brain areas of HIV-infected patients in the early stage, which suggested that cortical atrophy occurs in HIV infection during this period. This finding is consistent with most previous studies with MRI,[2,20,21,32] while it does not agree with several previous studies in perinatally HIV-infected adolescents.[22,31] Since all perinatally HIV-infected adolescents were receiving ART medication at the time of the MRI scan, the average age for initiation of any antiretroviral therapy was too long and considerable cerebral damage may have already occurred.[22] Anatomically, our results showed that decreased GM volume in the HIV infection group was mostly present in left frontal cortices. This finding was extremely consistent with the findings reported by Küper

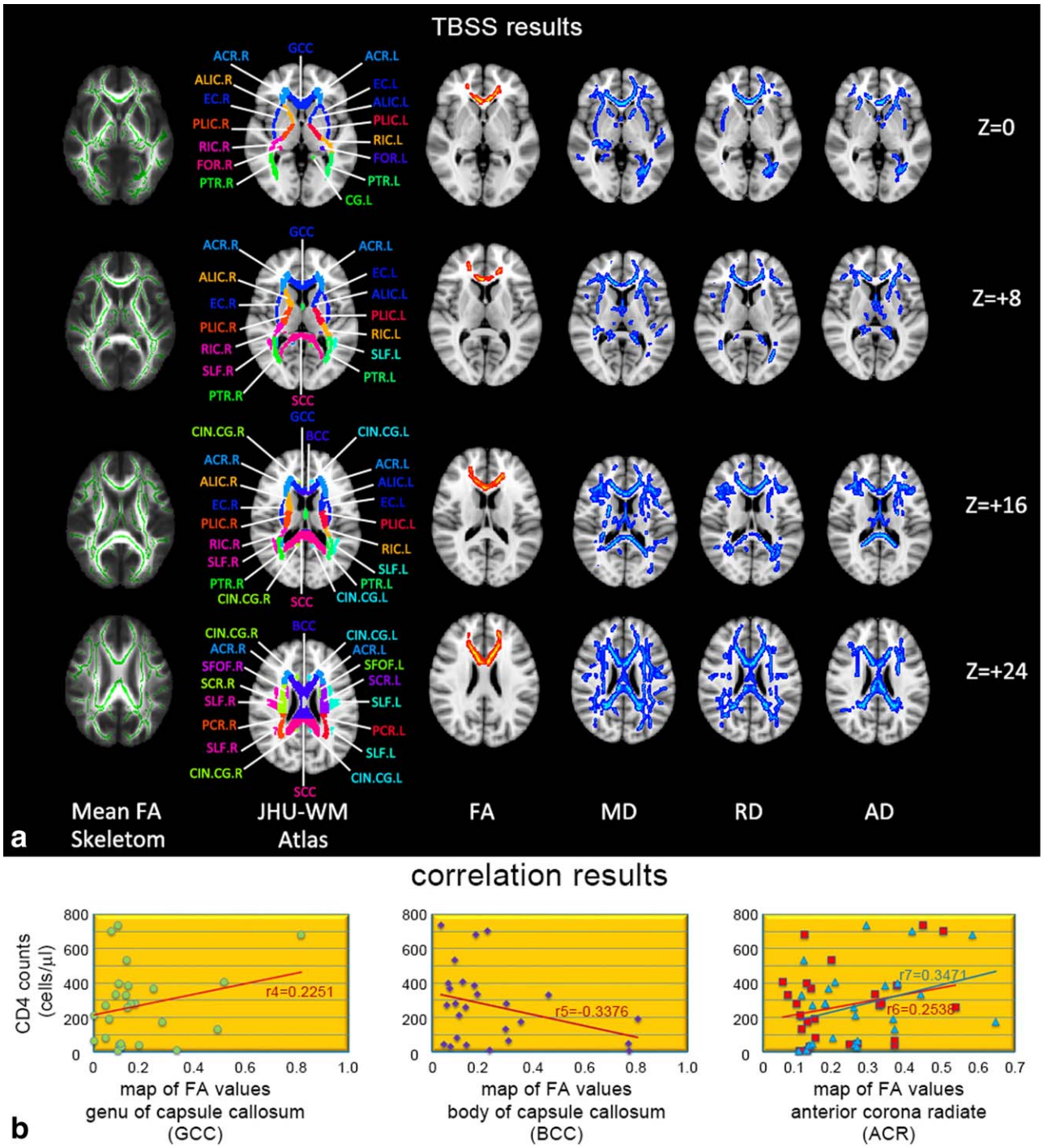

FIGURE 2: Tract-based spatial statistics (TBSS) analysis of voxel-wise group comparisons between the HIV infection and healthy control groups.

et al.[21] Changes in bilateral frontal GM in HIV infection have been reported in a previous morphometric study by Thompson et al.[32] Conversely, a functional (f)MRI study demonstrated that left temporal blood oxygenation-dependent (BOLD) signal increases occurred over the time course of 1 year during a visual attention task in neurocognitive-stable HIV patients.[33] It is well known that the frontal lobe is responsible for extensive cognitive function, such as long-term and working memory, awareness, and language sequencing, all of which may contribute to the impaired neuropsychological profile.[34] Although it is still unknown whether the brain can be protected or recover from early HIV-infection, our finding of decreased frontal cortices in this period may partly explain the failure of neuroprotection strategies initiated later in infection.[21]

Meanwhile, decreased GM volume in bilateral ACR in the HIV infection group was also found in our study when compared to the healthy controls. The VBM study by

TABLE 4. Location and Cluster Size (Clusters of > 100 Voxels) of Abnormal White Matter (WM) Tracts Between HIV-Infected Patients and Healthy Controls

WM structures (JHU-WM Atlas)	Size	HIV-infected patients vs. controls cluster size			
		FA	MD	RD	AD
GCC	-	1648	3034	3250	365
BCC	-	2751	2563	828	278
SCC	-	-	3505	2046	550
ACR	L	189	3934	3557	696
	R	238	4290	3835	905
EC	L	-	4028	-	747
	R	-	2506	1949	521
ALIC	L	-	3155	2387	798
	R	-	3019	-	913
PLIC	L	-	1606	365	531
	R	-	2511	-	-
RIC	L	-	2464	-	-
	R	-	3087	2592	-
PTR	L	-	2699	1983	1533
	R	-	2208	570	-
SLF	L	-	2841	2765	-
	R	-	2255	1364	-
CIN-CG	L	-	-	2339	-
	R	-	-	1500	-
FOR	-	-	244	227	195
SFOF	L	-	3421	3006	-
	R	-	2820	1988	-
SCR	L	-	1459	1267	259
	R	-	784	1218	102
PCR	L	-	3914	3011	878
	R	-	3631	2304	189
TPT	L	-	743	355	-
	R	-	436	132	-

The same abbreviations were used for all tables and figures: L, left; R, right; JHU-WM Atlas, the ICBM-DTI-81 White Matter Atlas; FA, fractional anisotropy; MD, mean diffusivity; RD, radial diffusivity; AD, axial diffusivity; -, unavailable; GCC, genu of corpus callosum; BCC, body of corpus callosum; SCC, splenium of corpus callosum; ACR, anterior corona radiate; EC, external capsule; ALIC, anterior limb of internal capsule; PLIC, posterior limb of internal capsule; RIC, retrolenticular part of internal capsule; PTR, posterior thalamic radiation; SLF, superior longitudinal fasciculus; CIN-CG, cingulum (cingulate gyrus); FOR, fornix (column and body of fornix); SFOF, superior fronto-occipital fasciculus; SCR, superior corona radiate; PCR, posterior corona radiate; TPT, tapetum.

Küper et al demonstrated GM tissue reduction in the ACR bilaterally, correlating with cognitive decline.[21] Similar alterations related to cognitive dysfunction were also reported in another study by Chiang et al.[35] Although strong evidence for the relationship between alteration in ACR and cognitive profile is lacking, our finding suggested that cognitive decline may have occurred in early HIV infection, even though symptoms are usually not present.[3]

For WM abnormalities in HIV infection, our TBSS results showed decreased FA in several WM regions, and more extensive WM regions with increased MD, RD, and AD in HIV-infected patients. These findings were generally consistent with previous HIV infection studies.[10–15] Importantly, using TBSS analysis our study provided evidence that the WM alterations occur in early HIV infection.

Most previous DTI studies in HIV infection have reported WM alterations in multiple brain regions, notably located in the corpus callosum, frontal WM, internal capsule, and corona radiate.[11–19] In our study, we only identified decreased FA in the GCC, BCC, and bilateral ACR,

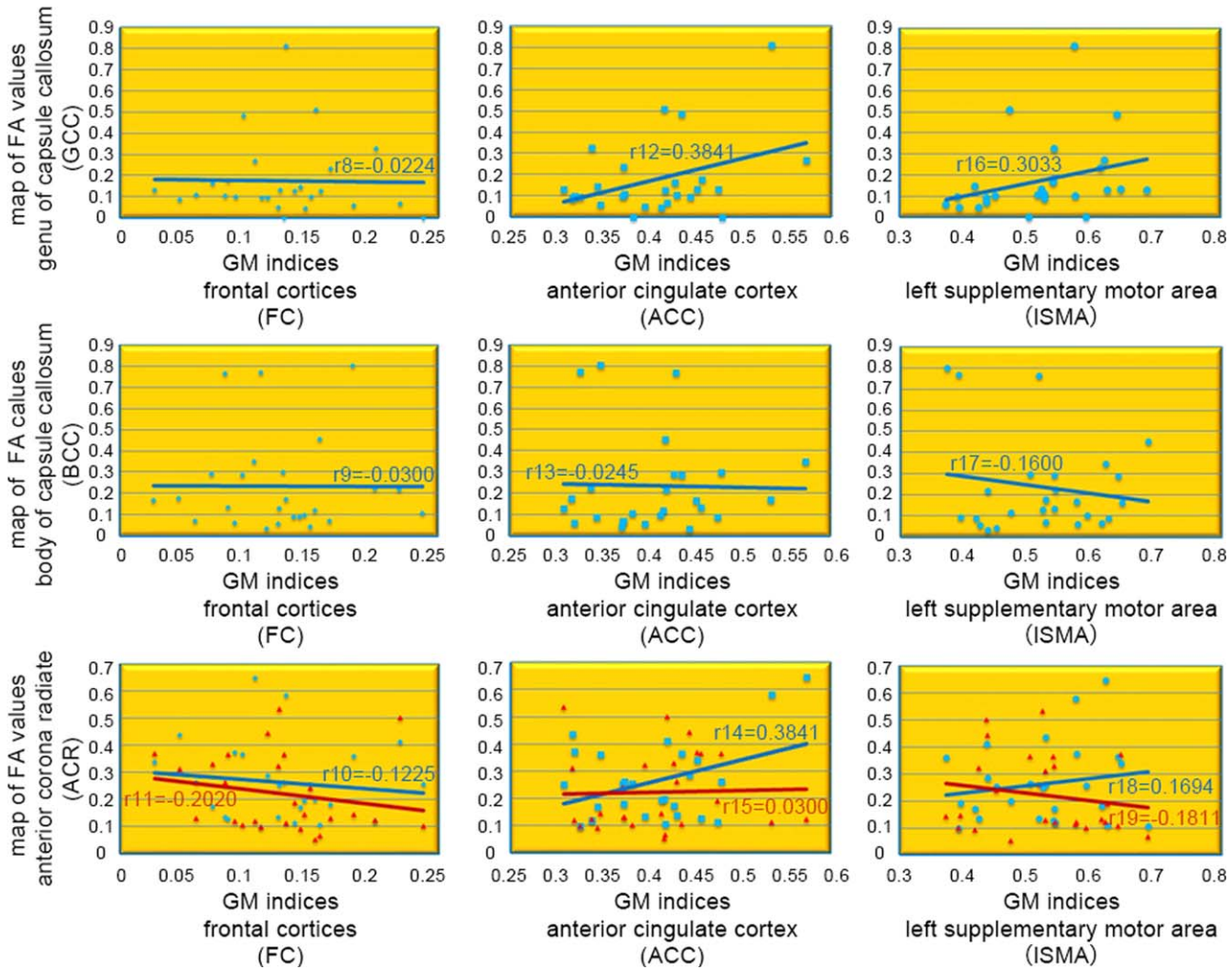

FIGURE 3: Correlations analysis between GM and WM abnormalities in the HIV-infected group.

which was consistent with a prior study.[37] Our findings may provide evidence that cognitive decline may occur in early HIV infection, even before symptoms appear.

Among four DTI parameters investigated in this study, simultaneous increases of MD, RD, and AD were present in more regions, similar to previous studies.[18,19] Moreover, it appeared that changes in MD and RD were more prominent than AD, which is extremely consistent with the findings reported by Zhu et al.[19] Previous animal model-based studies suggested that abnormalities in RD is a marker for demyelination.[38] Thus, our findings would imply that the inflammatory insult to the WM is predominantly demyelinating, while axonal injury co-occurs but to a lesser degree in the early HIV infection.

In our study we also investigated the relationship between GM changes and WM alterations. Unfortunately, there were no significant correlations between these two measures. This phenomenon suggested that the morphological changes in the early stage of HIV infection on the brain's GM and WM were not significantly linearly correlated, although abnormalities coexisted in both GM and WM.

Finally, there are several limitations of the current study that need to be considered. First of all, our results were limited to a small participant cohort, which may have an effect on the power of the statistical analysis in our study. Thus, more subjects are needed in further studies. Second, there was no neuropsychological testing in our study, so we cannot well analyze the association between cerebral cortex dysfunction and behavior patterns. The last inevitable limitation suffers from DTI's inherent artifacts and limitations. The partial volume effect and the inability of the model to cope with non-Gaussian diffusion are the two main drawbacks of DTI, which results in local registration errors during the TBSS's skeleton projection. Thus, a more accurate registration method should be considered to reduce the magnitude of such errors.

In conclusion, our cross-sectional study showed that HIV infection leads to structural regional brain abnormalities in the early period by using VBM and TBSS analysis. These changes included both GM and WM, which may contribute to the clinical picture of cognitive deterioration.

Acknowledgments

Contract grant sponsor: National Natural Science Foundation of China; contract grant numbers: 81501549, 81571649, 81571634, 61172167, 81227901, 61231004, 81171314; Contract grant sponsor: National Basic Research Program of China (973 Program); contract grant number: 2011CB707700; Contract grant sponsor: National High Technology Research and Development Program of China (863 Program); contract grant number: 2012AA021105; Contract grant sponsor: NSFC-NIH Biomedical collaborative research program; contract grant number: 81261120414; Contract grant sponsor: Beijing Natural Science Foundation; contract grant numbers: 4132080, 7132108; Contract grant sponsor: Fundamental Research Funds for the Central Universities; contract grant number: K13JB00170; Contract grant sponsor: Special Research Funds for the Capital Health Development; contract grant number: 2011-2018-01; Contract grant sponsor: Beijing Municipal Administration of Hospitals Clinical Medicine Development of Special Funding Support; contract grant number: ZYLX201511; Contract grant sponsor: Foundation of Heilongjiang Educational Committee; contract grant number: 12531119.

Data in this article were provided by the Beijing You'an Hospital of Capital Medical University. We thank them for their data collection work. The authors also thank all the anonymous reviewers for their kind comments.

References

1. Sepkowitz KA. AIDS — the first 20 years. N Engl J Med 2001;344:1764–1772.
2. Ragin AB, Du H, Ochs R, et al. Structural brain alterations can be detected early in HIV infection. Neurology 2012;79:2328–2334.
3. Masliah E, DeTeresa RM, Mallory ME, Hansen LA. Changes in pathological findings at autopsy in AIDS cases for the last 15 years. AIDS 2000;14:69–74.
4. Langford TD, Letendre SL, Larrea GJ, Masliah E. Changing patterns in the neuropathogenesis of HIV during the HAART era. Brain Pathol 2003;13:195–210.
5. Jernigan TL, Archibald SL, Fennema-Notestine C, et al. Clinical factors related to brain structure in HIV: the CHARTER study. J Neurovirol 2011;17:248–257.
6. Sevigny JJ, Albert SM, McDermott MP, et al. An evaluation of neurocognitive status and markers of immune activation as predictors of time to death in advanced HIV infection. Arch Neurol 2007;64:97–102.
7. Gonzalez-Scarano F, Martin-Garcia J. The neuropathogenesis of AIDS. Nat Rev Immunol 2005;5:69–81.
8. Masters MC, Ances BM. Role of neuroimaging in HIV-associated neurocognitive disorders. Semin Neurol 2014;34:89–102.
9. Assaf Y, Pasternak O. Diffusion tensor imaging (DTI)-based white matter mapping in brain research: a review. J Mol Neurosci 2008;34:51–61.
10. Thurnher MM, Castillo M, Stadler A, Rieger A, Schmid B, Sundgren PC. Diffusion-tensor MR imaging of the brain in human immunodeficiency virus-positive patients. AJNR Am J Neuroradiol 2005;26:2275–2281.
11. Lu CH, Chen HL, Chang WN, et al. Assessing the chronic neuropsychologic sequelae of human immunodeficiency virus-negative cryptococcal meningitis by using diffusion tensor imaging. AJNR Am J Neuroradiol 2011;32:1333–1339.
12. Leite SC, Corrêa DG, Doring TM, et al. Diffusion tensor MRI evaluation of the corona radiata, cingulate gyri, and corpus callosum in HIV patients. J Magn Reson Imaging 2013;38:488–1493.
13. Pomara N, Crandall DT, Choi SJ, Johnson G, Lim KO. White matter abnormalities in HIV-1 infection: a diffusion tensor imaging study. Psychiatry Res 2001;106:15–24.
14. Towgood KJ, Pitkanen M, Kulasegaram R, et al. Mapping the brain in younger and older asymptomatic HIV-1 men: frontal volume changes in the absence of other cortical or diffusion tensor abnormalities. Cortex 2012;48:230–241.
15. Chang L, Wong V, Nakama H, et al. Greater than age-related changes in brain diffusion of HIV patients after 1 year. J Neuroimmune Pharmacol 2008;3:265–274.
16. Ragin AB, Storey P, Cohen BA, Epstein LG, Edelman RR. Whole brain diffusion tensor imaging in HIV-associated cognitive impairment. AJNR Am J Neuroradiol 2004;25:195–200.
17. Stebbins GT, Smith CA, Bartt RE, et al. HIV-associated alterations in normal-appearing white matter: a voxel-wise diffusion tensor imaging study. J Acquir Immune Defic Syndr 2007;46:564–573.
18. Chen Y, An H, Zhu H, et al. White matter abnormalities revealed by diffusion tensor imaging in non-demented and demented HIV + patients. NeuroImage 2009;47:1154–1162.
19. Zhu T, Zhong J, Hu R, et al. Patterns of white matter injury in HIV infection after partial immune reconstitution: a DTI tract-based spatial statistics study. J Neurovirol 2013;19:10–23.
20. Ashburner J, Friston KJ. Voxel-based morphometry—the methods. Neuroimage 2000;11:805–821.
21. Küper M, Rabe K, Esser S, et al. Structural gray and white matter changes in patients with HIV. J Neurol 2011;258:1066–1075.
22. Sarma MK, Nagarajana R, Kellerb MA, et al. Regional brain gray and white matter changes in perinatally HIV-infected adolescents. NeuroImage Clin 2014;4:29–34.
23. Smith SM, Jenkinson M, Johansen-Berg H, et al. Tract-based spatial statistics: voxelwise analysis of multi-subject diffusion data. NeuroImage 2006;31:1487–1505.
24. Ashburner J, Friston K. Multimodal image coregistration and partitioning: a unified framework. NeuroImage 1997;6:209–217.
25. Good CD, Johnsrude IS, Ashburner J, Henson RN, Friston KJ, Frackowiak RS. A voxel-based morphometric study of ageing in 465 normal adult human brains. NeuroImage 2001;14:21–36.
26. Smith SM. Fast robust automated brain extraction. Hum Brain Mapp 2002;17:143–155.
27. Nucifora PGP, Verma R, Lee SK, Melhem ER. Diffusion-tensor MR imaging and tractography: exploring brain microstructure and connectivity. Radiology 2007;245:367–384.
28. Rueckert D, Sonoda LI, Hayes C, Hill DL, Leach MO, Hawkes DJ. Non-rigid registration using free-form deformations: Application to breast MR images. IEEE Trans Med Imaging 1999;18:712–721.
29. Smith SM, Nichols TE. Threshold-free cluster enhancement: addressing problems of smoothing, threshold dependence and localisation in cluster inference. NeuroImage 2009;44:83–98.
30. Mori S, Wakana S, Nagae-Poetscher LM, van Zijl PVM. MRI atlas of human white matter. Amsterdam: Elsevier; 2005.
31. Sowell ER, Thompson PM, Welcome SE, et al. Cortical abnormalities in children and adolescents with attention-deficit hyperactivity disorder. Lancet 2003;362:1699–1707.
32. Thompson PM, Dutton RA, Hayashi KM, et al. Thinning of the cerebral cortex visualized in HIV/AIDS reflects $CD4^+$ T lymphocyte decline. Proc Natl Acad Sci U S A 2005;102:15647–15652.

33. Ernst T, Yakupov R, Nakama H, et al. Declined neural efficiency in cognitively stable human immunodeficiency virus patients. Ann Neurol 2009;65:316–325.

34. Thothathiri M, Schwartz MF, Thompson-Schill SL. Selection for position: the role of left ventrolateral prefrontal cortex in sequencing language. Brain Lang 2010;113:28–38.

35. Chiang MC, Dutton RA, Hayashi KM, et al. 3D pattern of brain atrophy in HIV/AIDS visualized using tensor-based morphometry. NeuroImage 2007;34:44–60.

36. He CQ, Dum RP, Strick PL. Topographic organization of corticospinal projections from the frontal lobe: motor areas on the medial surface of the hemisphere. J Neurosici 1995;15:3284–3306.

37. Stubbe-Dräger B, Deppe M, Mohammadi S, et al. Early microstructural white matter changes in patients with HIV: a diffusion tensor imaging study. BMC Neurol 2012;12:23.

38. MacDonald CL, Dikranian K, Bayly P, Holtzman D, Brody D. Diffusion tensor imaging reliably detects experimental traumatic axonal injury and indicates approximate time of injury. J Neurosci 2007;27:11869–11876.